Thermal Performance of Thermal Pad Contact Heat Exchangers

G. P. Peterson* and L. S. Fletcher†
Texas A&M University, College Station, Texas 77843
and
David Blackler‡
Rockwell International Corporation, Canoga Park, California 91303

An experimental investigation was conducted to determine the effect of variations in the load configuration and the resulting pressure distribution, on the thermal contact conductance of two 12.70 × 17.78 × 2.54 cm (5 × 7 × 1 in.) aluminum 6061-T6 surfaces. Four load configurations consisting of 4×4, 4×6, 5×7, and 6×8 arays were evaluated. A self-contained, general-purpose finite element program (ANSYS) and a relatively new pressure-sensitive film were used to determine the pressure distribution as a function of the total applied load. The 5 × 7 array was found to minimize the number of load points yet provide optimum thermal characteristics. Using this load configuration, a second set of experiments was conducted to determine the degree to which the thermal contact conductance could be enhanced through the application of selected coatings. Three coating materials were evaluated, a 2.5 μm thick layer of indium, a molybdenum disulfide coating (Moly-Tiolub-1175) 1.25 μm thick, and a Teflon impregnated anodized coating (Hard-Tuf X20) 1.25 μm thick. The results indicated that the thermal contact conductance of the thermal test pads could be enhanced by a factor of almost four by adding a coating of indium approximately 2.5 μm thick on one surface. The Moly-Tiolub-1175 and Hard-Tuf X20 coatings, while providing a somewhat more durable surface than indium, resulted in reductions in the thermal contact conductance of approximately 65% and 77%, respectively.

Introduction

IN order to provide for optimum thermal performance of Space Station Freedom, a large number of the electronic modules will be mounted externally and attached to a primary cooling loop. A traditional attachment technique involves bolting the electronic modules to a heat sink or cold plate.[1] An alternative method involves the use of thermal pads as a means for cooling and facilitating replacement of the malfunctioning modules. The electronic module, or orbital replacement unit (ORU), would be attached to one thermal pad with interior heat pipes that would be mated to a second thermal pad with a series of internal channels through which a coolant will be circulated.[2,3] The interface between the thermal pads, then, becomes the primary resistance to heat removal from the electronic modules.

When two smooth, nominally flat surfaces are brought together, they contact only in a relatively few discrete points, due to individual surface roughnesses and microscopic asperities.[4] Heat can be transferred across the interface by conduction through the metal-to-metal contacts, conduction through the substance in the gaps around the contact, radiation across the gap, or a combination of the three. In the application of interest here, conduction through the solid contacts is the dominant mode because convection is essentially zero due to the vacuum environment of space, and radiation is negligible due to the relatively low temperature gradient present at the interface. The other parameters that affect the thermal contact conductance of metallic interfaces include the following[5]: applied pressure, surface geometry, gap thickness, interstitial fluid, thermal conductivity, hardness, modulus of elasticity, and average interface temperature.

The most common method of enhancing the thermal contact conductance is to increase the apparent contact pressure. Unfortunately, this is not always possible due to design or load restrictions. In situations where the applied load is limited, as in the thermal pads, the thermal contact conductance can be enhanced through the use of thermally conductive greases, thin metal foils, or a thin metallic coating deposited on one or both of the contacting surfaces. In all of these situations, the interface material flows into the gaps between the two surfaces and increases the actual contact area, which in turn increases the thermal contact conductance.

Thermal greases are the most desirable of these three techniques for general applications. However, they tend to migrate at high temperatures or vaporize in low pressure or vacuum environments. Once vaporized, they may redeposit on adjoining surfaces or disappear altogether. Metal foils are theoretically very attractive but must be very thin to be effective and as a result, have a tendency to be difficult to handle. If not properly applied, these foils may result in decreases in the thermal contact conductance due to wrinkles or folds.

Although the physical phenomena involved in the use of thin metallic coatings to enhance the thermal contact conductance is not well understood, metallic coatings have several desirable characteristics. First, they are relatively easy to handle once applied and will not wrinkle or fold; second, under normal operating conditions they are unstable in a vacuum environment; and third, the vapor deposition, sputtering, and/or electroplating processes used to apply these coatings allow thin layers of almost any metal or combination of metals to be deposited in the desired thicknesses.

Several experimental and analytical investigations have explored the effect of thin metallic coatings on the thermal contact conductance at the interface of metallic surfaces. Fried and Kelly[6] compared the measured thermal contact conductance of uncoated stainless steel surfaces in a vacuum to that obtained when one of the stainless steel surfaces had been

Received May 21, 1990; presented as Paper 91-0364 at the AIAA 29th Aerospace Science Conference, Reno NV, Jan. 7–10, 1991; revision received April 12, 1991; accepted for publication April 28, 1991.

*Professor of Mechanical Engineering. Associate Fellow AIAA.
†Dietz Professor of Mechanical Engineering. Fellow AIAA.
‡Manager, Rocketdyne Division.

coated with a thin layer of vapor deposited aluminum. This comparison indicated that the overall joint conductance of uncoated junctions could be enhanced through the use of a coating material that was softer than the substrate.

Shortly after the completion of this work, Mal'kov and Dobashin[7] compared the overall joint conductance of two uncoated stainless steel surfaces in which one of the surfaces was then coated with silver. These tests, which were conducted in a vacuum, indicated a significant increase in the measured conductance values. This increase was found to decrease with respect to increases in the apparent interface pressure. In a later investigation,[8] the results of an experimental investigation that compared the overall joint conductance of uncoated bronze surfaces with those obtained when one bronze surface had been coated with a thin layer of a tin/nickel alloy were presented. Again it was observed that coating one surface increased the overall joint conductance significantly; however, the magnitude of this increase was found to decrease with respect to increases in the apparent interface pressure.

The analytical evaluation of the thermal contact conductance of thin metallic layers on metallic surfaces requires the simultaneous solution of three separate problems; the thermal problem, in which the questions of constriction resistance and thermal behavior must be addressed; the mechanical problem, in which the various physical properties such as surface hardness and elastic modulus must be addressed; and the metrological problem, in which the effects of the surface characteristics such as roughness, waviness, flatness, and asperity slope must be addressed.[4]

Although not addressing all of these issues, Al-Astrabadi et al.[9] developed an analytical model for predicting the contact conductance of tin coated stainless steel interfaces and compared the results with those of their own experimental investigation. The resulting large variations between the predicted and measured values were partially due to the difference in the analytical method, which predicted the thermal contact conductance, and the experimental tests, which were used to measure the conductance. In the analytical investigation, the constriction resistance resulting from a reduction in the actual contact area was predicted while in the experimental tests, the overall joint resistance, composed of the summation of the thermal contact conductance, and the bulk resistance of the metallic coating material, was measured. The thermal problem also has been addressed[10] along with the mechanical and metrological issues.[11]

Two recent investigations[12,13] addressed all three of these issues, the thermal problem, the mechanical analysis, and the metrological problem, simultaneously. In a combined analytical and experimental investigation[12] the thermal contact conductance of nickel surfaces coated with thin metallic layers of silver were investigated. In the analytical portion, the coated metallic interface was reduced to an equivalent uncoated metal interface by using the concepts of effective hardness, effective thermal conductivity, and an uncoated interface correlation developed previously. The predicted thermal contact conductance values were compared with the results of an experimental investigation in which several nickel surfaces were coated with varying thicknesses of vapor deposited silver. The contact conductance was shown to increase at a relatively constant rate, approximately twice as large as that observed in the bronze or stainless steel surfaces previously reported. In addition, evidence of an optimum coating thickness was presented and it was proposed that this optimum thickness was dependent on the hardness/conductivity ratio.

The most extensive investigation of different types and thicknesses of metallic coatings was conducted by Kang et al.[13] This study included an experimental investigation to determine the extent to which the thermal contact conductance at the interface of contacting Aluminum 6061-T6 interfaces could be enhanced through the use of vapor deposited metallic coatings. Three different coating materials, lead, tin, and indium, were evaluated using four different thicknesses for each coating material. The results verified the existence of an optimum coating thickness, demonstrated that the percentage increase in the overall joint conductance was strongly pressure dependent, and found that the hardness of the coating material was the most significant parameter in the ranking of the substrate and coating material combinations for the surfaces investigated.

The performance of the thermal pad configuration is largely dependent upon the thermal resistance occurring at the interface between the two thermal pads. This thermal contact resistance is in turn dependent upon several parameters, most important of which are the overall pressure occurring at this interface (total load divided by thermal pad area) and the distribution of that pressure.[14,15]

The objective of the present investigation was twofold: First to determine the effect of variations in the load configuration and the resulting pressure distribution on the thermal contact conductance and second, to determine the degree to which the thermal contact conductance at the interface of two 12.70 × 17.78 × 2.54 cm (5 × 7 × 1 in.) Aluminum 6061-T6 surfaces could be enhanced through the application of thin coatings.

Pressure Distribution Evaluation

To determine the effect of variations in the number and location of loading points on the interface pressure of the two thermal test pads, a numerical model was developed. This model utilized ANSYS,* a self-contained general purpose finite element program. Load configurations of 4 × 4, 4 × 6, 5 × 7, and 6 × 8 arrays of equally distributed load points were evaluated to determine what effect these parameters had on the distribution and magnitude of the load at the interface. In this way, the thermal pad load distribution and pressure could be quantified and optimized.

Numerical Model

Three-dimensional, isoparametric solid cubic elements were used in the numerical model with each element incorporating a total of eight node points, one at each corner of the cubic element. Because the force distribution on the thermal test pad was in a structured array, symmetry about the central axes was assumed and it was necessary to model only one-quarter of the test pad, as illustrated in Fig. 1. A zero displacement boundary condition was employed at the interface directly between the two loading points. In order to have the loads concentrated at the proper nodes, it was necessary to use a different nodal distribution for each of the four load configurations.

Using this model and several different total loads, the pressure variation at the test pad interface was determined for the 5 × 7 array. The results of these tests indicated that the interface pressure variation was directly proportional to the total load. For this reason, the remaining numerical tests focused on total loads of either 18.7 kN (827.4 kPa) or 37.4 kN (1.7 MPa).

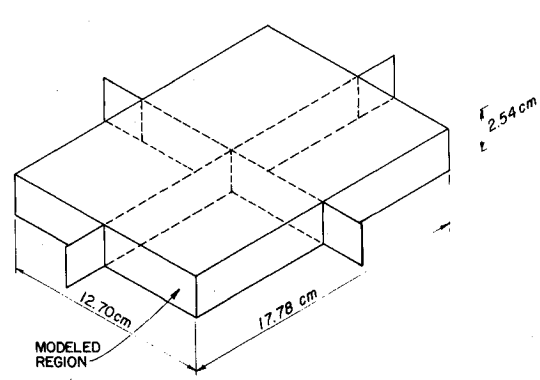

Fig. 1 Numerically modeled region.

Table 1 Thermal test pad surface characteristics

	Specimen number						
	$R_a(\mu in.)$	$R_t(\mu in.)$	$R_q(\mu in.)$	R_{da}	R_{dq}	$W_a(\mu in.)$	$W_t(\mu in.)$
	Pressure test surfaces						
Plate A	0.36	4.31	0.47	0.091	0.117	0.10	1.09
Plate B	0.32	3.12	0.41	0.072	0.093	0.13	0.97
	Heat transfer test surfaces						
1A	12.2	146.7	16.3	0.075	0.100	4	27
1B	15.7	170.7	21.5	0.085	0.112	17	71
2A	12.5	118.2	16.5	0.076	0.098	5	32
2B	13.5	187.5	18.8	0.079	0.103	5	29
3A	10.0	99.2	13.0	0.057	0.077	5	32
3B	11.2	133.7	14.7	0.061	0.083	5	33
4A	12.7	137.2	17.2	0.074	0.099	4	28
4B	12.5	129.5	16.5	0.078	0.103	5	33
5A	10.7	140.5	14.5	0.062	0.084	4	30
5B	12.5	135.2	16.5	0.070	0.092	5	44
6A	13.2	134.2	17.0	0.070	0.095	5	34
6B	13.7	149.7	18.2	0.082	0.106	8	64
7A	14.2	169.8	18.5	0.091	0.117	4	43
7B	12.5	122.7	16.3	0.072	0.093	5	38

R_a = Arithmetic average roughness; R_t = peak to valley height; R_q = rms roughness; R_{da} = arithmetic average asperity slope; R_{dq} = rms asperity slope; W_a = arithmetic average waviness height; W_t = maximum waviness height.

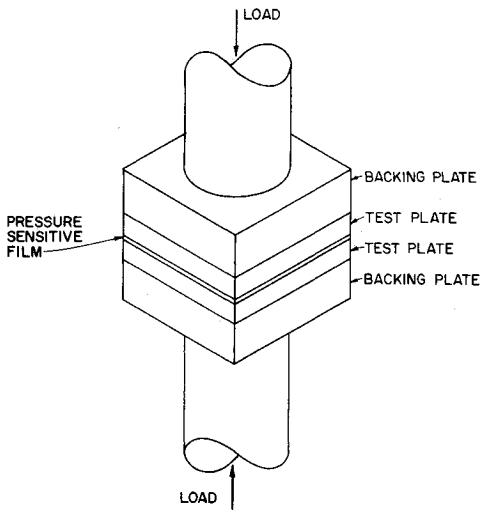

Fig. 2 Load distribution test facility.

As illustrated, the interface pressure variation is directly proportional to the total load, i.e., the pressure for the 37.4 kN (8400 lb) load is twice that for the 18.7 kN (4200 lb) load, and the pressure variation decreases with an increase in the number of load points. The pressure variation for the 37.4 kN (8400 lb) load ranges from 0 to 3.2 MPa (0 to 466.9 psi) for the 4 × 4 configuration and 1.3 to 1.9 MPa (183.10 to 271.15 psi) for the 6 × 8 configuration, while for the 18.7 kN (4200 lb) load the variation ranges from 0 to 1.6 MPa (0 to 233.44 psi) for the 4 × 4 configuration and 0.6 to 0.9 MPa (91.55 to 135.58 psi) for the 6 × 8 configuration.

Pressure Measurement

An Instron Universal Testing Machine, Model 4206 was used in the experimental investigation to determine the effect of the load configuration on the pressure at the interface of two thermal test pads. One set of thermal test pads 12.70 × 17.78 × 2.54 cm (5 × 7 × 1 in.) were prepared from a single piece of Aluminum 6061-T6. Once fabricated, the test pads were sent to Massey Grinding Services in Houston, Texas, where the contacting surfaces were ground to a smooth flat finish. Upon completion of the grinding, the test pads were sent to Sheffield Measurements Laboratory in Dayton, Ohio where the surface parameters, including the RMS roughness, CLA roughness, average peak to valley height, arithmetic average asperity slope, RMS asperity slope, and arithmetic average waviness were measured. The surface finish for each of the two thermal test pads is shown in Table 1 and was approximately 1.778 μm RMS. Flatness deviation and parallel tolerances of less than 1.778 μm (0.0007 in.) and 1.778 μm (0.0007 in.), respectively, were maintained for both of the test pads.

The experimental load facility shown in Fig. 2, was arranged to ensure that the axial load and alignment could be closely controlled and monitored. In addition to the Instron machine and two test plates, two backing plates and four sets of load distribution plates were prepared. The two backing plates were constructed from cold rolled steel and both the upper and lower surfaces were ground in a manner similar to that used for the test pads. The surface flatness deviation was held to less than 1.778 μm (0.0007 in.) and the two contacting surfaces were held parallel to within 1.778 μm (0.0007 in.). The purpose of the two backing plates was to ensure that the load resulting from the 12.70-cm (5 in.) diameter Instron pressure ram was uniformly distributed.

In order to obtain the desired load distributions, four sets of load distribution plates were constructed. Each set consisted of two plates, one pin plate and one plate using Bellville washers, i.e., conical shaped springs. The pin plate was constructed from 0.635-cm (0.25 in.) thick, cold rolled steel and had a series of ceramic pins 0.635 cm (0.25 in.) in diameter and .0525 cm (0.375 in.) in length, located at each load point. The Bellville washer plate was also made from 0.625-cm (0.25 in.) cold rolled steel and had locating holes 7.62 μm (0.003 in.) deep machined into one side at each load point. Once these load distribution plates had been machined, they were surface ground to the same tolerances at the two backing plates.

To measure the pressure variation at the interface, two types of Fuji Prescale Pressure-Sensitive Film® (Super Low Pressure and Low Pressure) are used. The recommended pressure ranges of these films are 71 to 284 kPa and 285 to 994 kPa, respectively, making them adequate for use in the present investigation. The developed film was read using a Fuji Densitometer, Model #FJ35,® which, by measuring the density of the color of the film, gave a digital reading of the interface pressure.

By combining the plates described above into a vertical stack consisting of one backing plate, the pin plate, the two test plates, the Bellville washer plate, and the other backing

plate, and installing this stack in the Instron, the magnitude and distribution of the load could be controlled. The interface pressure distribution was measured using the pressure-sensitive film for a total of five different configurations, a uniform pressure distribution, 4 × 4 array, a 4 × 6 array, a 5 × 7 array, and a 6 × 8 array. Because the numerical model described previously indicated that for a given configuration, variations in the interface pressure were directly proportional to the overall load, measurements were made at only two loads for each configuration.

Prior to the tests, the two backing plates were loaded and a 15.24 × 20.32 cm (6 × 8 in.) sheet of the pressure-sensitive film was placed between them. Loads of 18.7 kN (4200 lb) and 37.4 kN (8400 lb) were applied and held for approximately 5 min in order to develop the film and obtain baseline values. Several such tests were conducted to assure repeatability and determine the variation in the pressure distribution for the uniformly loaded plates.

Following these calibration tests, one of the sets of load configuration plates, which consisted of the pin plate and the Bellville washer plate, were added to the stack—one above and one below the test pads. The two test pads were then brought into contact and held at a load of 18.7 kN (4200 lb) for a minimum of 5 min while the film was developed. The test pads were then separated and the exposed film removed. The resulting pressure distribution was recorded and the process repeated for a load of 37.4 kN (8400 lb). This procedure was repeated until all four load configurations had been evaluated.

Once developed, the interface pressure distribution was measured using the densitometer. Experimental data were taken over only one-quarter of the plate (as shown in Fig. 1) and the number of data points varied from 63 for the 4 × 4 load configuration to 163 for the 6 x 8 load configuration. For each point, a total of four readings were taken and averaged. The reading from the densitometer was then converted to pressure using the expression

$$P = (0.856714 + 20.8976\mathrm{D} - 26.7382D^2 + 23.738D^4)(97.9) \quad (1)$$

where P is in kPa and D is the densitometer reading. In this manner, a digitized interface pressure distribution map was constructed for comparison with the results obtained from the numerical model.

Thermal Conductance Evaluation

All of the thermal contact conductance tests were performed using a specially designed test fixture, shown in Fig. 3, installed in a high vacuum thermal contact conductance test facility. The pressure in this facility was maintained to a vacuum of less than 10^{-5} Torr by an Alcatel 2300 C roughing pump in series with a VHS-6 Oil Diffusion Pump. The vacuum was measured with an ion gage tube and controller. The thermal contact conductance test fixture was comprised of a vertical stack consisting of the lower frame plate, the lower Bellville washer plate, a cooling plate, the lower thermal test pad, the upper thermal test pad, a silicone rubber heater, the upper support pin plate, the load distribution plate, a 0–22.24 kN (0–5000 lb) load cell, and a diaphragm cylinder mounted on the upper frame plate. In order to have the two thermal test pads separated during the initial pump down, the upper portion of the stack (the upper thermal test pad, the silicone rubber heater, the upper support pin plate, and the load distribution plate) were held together by thin Teflon straps.

Three cold plates, one for each load configuration, were constructed from aluminum and were maintained at the required temperature by a coolant circulated through a constant temperature circulating bath. The internal configuration of each cold plate was constructed with lands located directly opposite the loading pins and Bellville washers. These lands

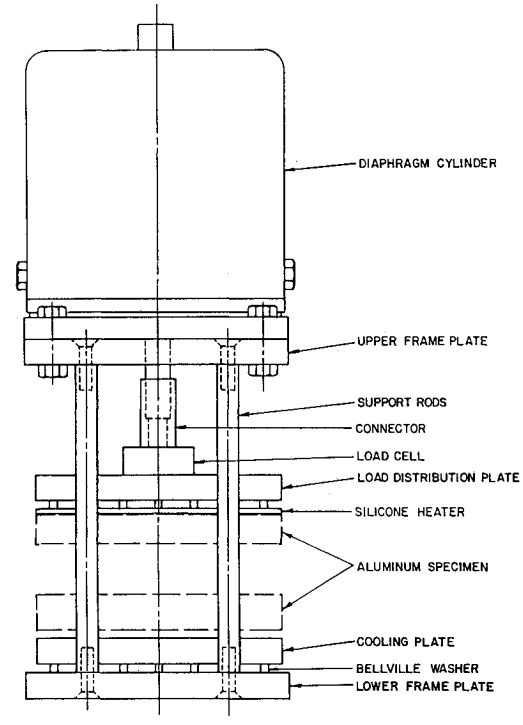

Fig. 3 Thermal pad contact conductance test facility.

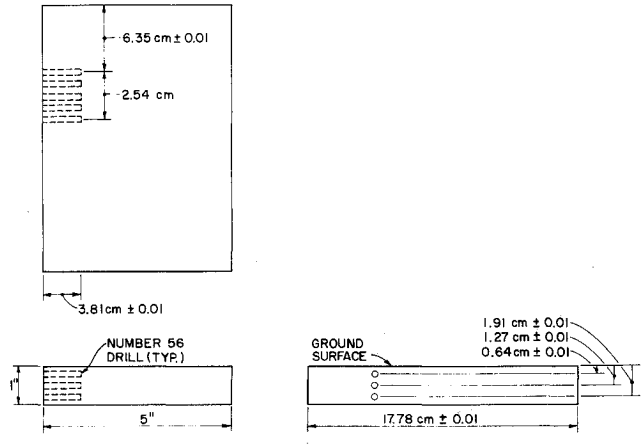

Fig. 4 Thermal pads.

allowed the force from the support pins and washers to be transmitted directly through the cold plates with a minimal amount of distortion to the loading pattern. The interface between the cold plate and the lower thermal test pad was coated with a thermally conductive grease (Dow Corning 340 Compound®) to minimize the thermal resistance at the interface.

Experimental Test Articles

The upper and lower thermal test pads were identical and were constructed from Aluminum 6061-T6. Five sets of three thermocouple wells were drilled in each thermal test pad. The three thermocouples in each set were spaced at 6.35-mm intervals through the thickness of each plate as shown in Fig. 4. On each thermal test pad, these five sets of thermocouples were used to determine the variation in the thermal contact conductance at the interface of the two thermal test pads. An internal region between two centrally located support points on the 5 × 7 array was selected and instrumented with these five sets of thermocouples. On each test pad, one set of thermocouples was located at the centerline of each of two adjoining support points in the 5 × 7 array. The remaining three

sets of thermocouples were located at equal distances between the two load point centerlines. One K-type thermocouple (AWG 30) was cemented into each thermocouple well using a thermally conductive epoxy. In this manner, the local thermal contact conductance could be computed as a function of the distance from a given support pin centerline. The same instrumentation technique was used for the 4 × 6 and 6 × 8 load configurations, but because the pin locations were different, the thermocouples were not spaced evenly between the support points.

Heat was provided by a 12.70 × 17.78 cm, 120-V silicone rubber resistance heater manufactured and attached to the top surface of the upper thermal test pad. These heaters had a maximum heat flux capacity of 2.32 W/cm^2 and were attached using a silicone adhesive. Power to the heater was provided by a variable voltage power supply and measured by monitoring the voltage and current supplied to the heater. However, because the location of the thermocouples and the thermal conductivity of the test pads were known, the heat flux could be computed directly and the measured values were used only as a check.

Experimental Procedure

Prior to the thermal contact conductance tests, a 2.54-cm-diameter, 2.54-cm-long sample of the material from which the thermal test plates were fabricated was evaluated to determine the temperature dependence thermal conductivity. The procedure used has been described previously[13] and resulted in the following expressions:

$$k_u = 111.94 + 0.226 \times T_u \quad (2)$$

and

$$k_L = 111.94 + 0.226 \times T_L \quad (3)$$

where k_u and k_L are the thermal conductivity of the upper and lower plate, respectively. Extrapolation of the measured temperatures to the interface resulted in surface temperatures at five discrete points on the surface. Dividing the local heat flux Q/A by the difference in the two surface temperatures, resulted in a value for the local thermal contact conductance. This method has previously been shown to be far superior to bulk measurements obtained by measuring the total input power and the overall temperature drop across the thermal test pads. In addition, the present method provided by which the thermal contact conductance at selected locations could be determined rather than a bulk value.

To determine the effect of the load configuration on the thermal contact conductance, six sets of thermal test pads, 12.70 × 17.78 × 2.54 cm, were prepared from a single piece of Aluminum 6061-T6, as shown in Fig. 4. Once machined and ground, the surface parameters, including the RMS roughness, CLA roughness, average peak to valley height, arithmetic average asperity slope, RMS asperity slope, and arithmetic average waviness were measured. The results of these measurements are summarized in Table 1. Upon completion of the surface characteristics each thermal test pad was instrumented with a total of 15 AWG-30 K-type thermocouples and the silicone heater was attached to the backside of one thermal test pad from each set. Each of the five sets of thermal pads were then placed in the test fixture and loaded with a force of 20.24 kN. This preloading resulted in an apparent interface pressure of 896 kPa (130 psi) and was necessary to reduce the effect of variations resulting from plastic deformation ofthe asperities. Because of large variations in the surface characteristics one set, TTPS-1, was used to refine the test procedure and therefore no data are reported for this set.

After completion of the preloading, a set of experiments were conducted on TTPS-2 to determine the effect of variations in the loading configuration. Three different load configurations were evaluated, a 4 × 6, 5 × 7, and 6 × 8 array. The procedure followed for all of the thermal contact conductance tests was to install a set of thermal test pads in the test fixture along with the cooling plate, pin pressure plate, and Bellville washer plate for one of the three load configurations and to then connect the thermocouples and heater. Once the heater and thermocouples had been checked for proper operation, the two contacting surfaces were aligned, wiped clean with acetone, and the chamber evacuated to a pressure of less than 10^{-5} Torr. After evacuation, the two plates were brought into contact by pressurizing the load cylinder to a pressure sufficient to result in an apparent interface pressure of 206.8 kPa (30 psi).

Once steady-state conditions had been reached, data were taken and the load was incremented to achieve apparent interface pressures of 206.8, 344.7, 551.6, 689.5, and 827.4 kPa (30, 50, 80, 100, and 120 psi). Throughout all of the tests, the power to the heater and the temperature of the constant temperature circulating bath were adjusted to maintain an average interface temperature of 300 K ± 5 K.

After evaluation of the thermal contact conductance of the various load configurations had been completed, a series of tests were conducted to determine the degree to which the thermal contact conductance at the interface of the two Aluminum 6061-T6 surfaces could be enhanced through the application of thin coating materials. Three different coatings were evaluated, a pure indium coating 2.5 μm thick, a molybdenum disulfide coating (Moly-Tiolub-1175) 1.25 μm thick, and a Teflon impregnated anodized coating (Hard-Tuf X20) 1.25 μm thick.

Prior to testing the coated test pads, three sets of uncoated thermal test pads, TTP-2, 3, and 4, were evaluated at a pressure of 689.5 kPa (100 psi) using the 5 × 7 load configuration, to establish a baseline conductance from which the relative improvements of the different coatings could be measured. The test procedure followed for these tests was identical to that described previously.

After the thermal contact conductance of each of the uncoated sets had been measured, one test pad from each set (the one without the heater) was coated. One test pad from TTPS-2, was sent to Thin Film Technology in Buelton, California, where the contacting surface was coated with a 2.5-μm layer of indium. Two other test pads, TTPS-3 and 4, were sent to Tiodize Inc. in Huntington Beach, California where the contacting surfaces were coated with a molybdenum disulfide coating (Moly-Tiolub-1175) 1.25 μm thick and a Teflon impregnated anodized coating (Hard-Tuf X20) 1.25 μm thick, respectively.

Results and Discussion

For clarity, the experimental results are presented in two distinct sections, those resulting from the pressure distribution and those resulting from the thermal conductance tests.

Pressure Distribution

The numerically determined pressure variations for the thermal test pads were evaluated for all load configurations, and are shown in Figs. 5a and 5b for the 5 × 7 load array for 18.683 kN and 37.365 kN. These two-dimensional pressure variations clearly demonstrate the calculated symmetry of the imposed load distribution points. A careful analysis of Fig. 5a suggests that for the 18.7 kN (4200 lb) load, the pressure gradients are not significant because the larger number of loading points provides more uniform loading, as demonstrated by the increased spacing between constant pressure lines. For the 37.4 kN (8400 lb) load, the 5 × 7 array configuration results in a moderate pressure variation with a fairly uniform pressure distribution across the thermal test pad.

Figures 6a and 6b illustrate the experimentally obtained pressure distribution resulting from the conversion of the densitometer readings obtained for the thermal test pads with a uniform load of 18.7 kN (4200 lb) and 37.4 kN (8400 lb),

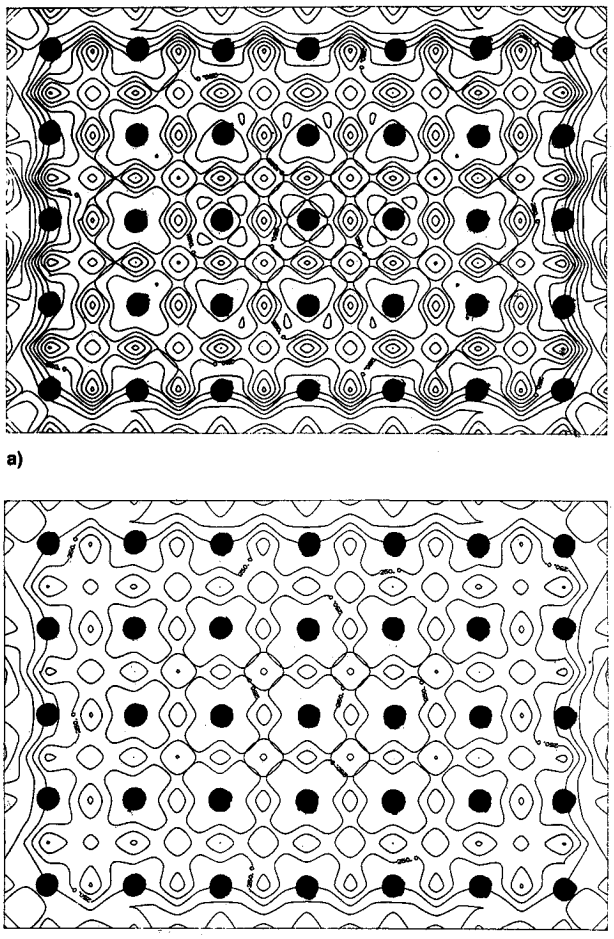

Fig. 5 Numerically obtained pressure distribution for the 5 × 7 configuration at: a) 18.7 kN load; b) 37.4 kN load.

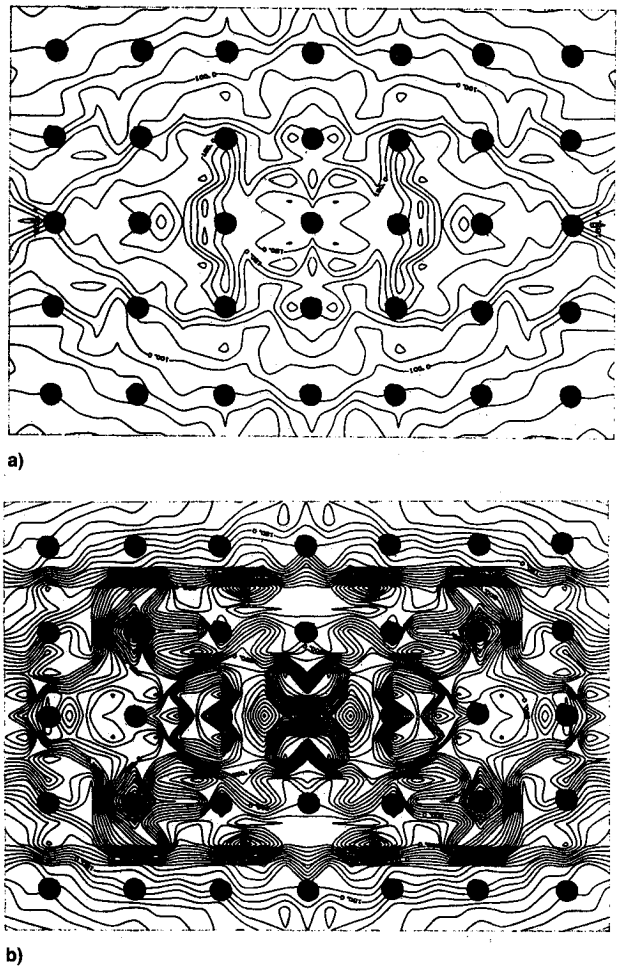

Fig. 6 Experimental results for the 5 × 7 configuration at: a) 18.7 kN load; b) 37.4 kN load.

respectively. For comparative purposes, pressure increments of 68.9 kPa (10 psi) were used for both the 18.7 kN (4200 lb) load and the 37.4 kN (8400 lb) load.

Although the numerically determined pressure variation provides a reasonable interface pressure distribution map, and demonstrate the importance of selecting the optimum array of loading points, the experimentally obtained pressure distribution resulting from the different load configurations did not demonstrate as uniform a pattern as might be expected, for either the 18.7 kN (4200 lb) load or for the 37.4 kN (8400 lb) load. Although resurfacing of the backing plates and test pads resulted in some improvement, it was not possible to obtain a completely uniform initial pressure distribution. The correlation between the experimental and numerical model, however, is adequate to provide verification of the numerical model.

Thermal Pad Conductance

Table 2 contains a summary of the thermal pad conductance data for the 4 × 6, 5 × 7, and 6 × 8 load configurations, and these data are illustrated graphically in Fig. 7. As shown, the thermal contact conductance is dependent upon both the load configuration and the apparent interface pressure.

By combining each of the measured thermal contact conductance values for a given load configuration with the apparent contact pressure, an expression for the thermal contact conductance as a function of radial distance from the loading points was obtained. Assuming symmetry around each load point and defining a unit cell as the region bounded by the line midway between each load point, these expressions were integrated and then multiplied by the total number of load points to obtain the overall plate conductance. Table 3 illustrates the results of this process for the load configuration tests. As shown, the integrated values vary considerably with the highest values occurring for the 6 × 8 array. At an apparent pressure of 689.5 kPa (100 psi), the integrated value for the 5 × 7 array is 33.7% higher than for the 4 × 6 array while the value of the 6 × 8 array is only 4.4% higher than for the 5 × 7 array. This trend holds true for all of the pressures tested and indicates that although increasing the number of load points improves the conductance there is only minimal improvement between the 5 × 7 array and the 6 × 8 array.

As discussed previously, in order to determine the extent to which the thermal contact conductance could be enhanced by the addition of thin coating materials TTPS-3, -4, and -5 were first tested with no coating, then coated and retested. The results of the tests to determine the effect of the coating materials are illustrated in Fig. 8. The dimensionless conductance, shown as the ordinate, is expressed as the ratio of the coated thermal contact conductance to the uncoated thermal contact conductance and is presented as a function of distance from a local point. As shown, the indium coating resulted in an almost constant enhancement factor of approximately 4. The Moly-Tiolub-1175 and Hard-Tuf X20 coated interfaces, however, both significantly reduced the thermal conductance. In general, the Moly-Tiolub-1175 coating reduced the thermal contact conductance by approximately 65%, whereas the Hard-Tuf X20 coating resulted in a reduction of from 69% to 82%, depending upon the location of the measurement.

Table 2 Load configuration thermal contact conductance data (set 2)

Distance from pin CL, (mm)	Interface Pressure				
	206.8 kPa	244.7 kPa	551.6 kPa	689.5 kPa	827.4 kPa
			4 × 6 Array		
9.76	211.30	441.53	1089.25	2113.28	3618.08
10.42	200.60	419.48	1047.33	2023.66	3577.83
12.02	182.49	430.61	1012.15	1891.66	3547.53
12.74	167.50	402.98	1028.59	1932.11	3528.53
14.24	164.93	358.54	961.70	1773.41	3486.10
			5 × 7 Array		
0.00	459.29	666.26	1658.48	3172.15	5565.53
6.35	388.84	586.13	1522.06	2941.49	4797.40
12.70	372.22	557.29	1460.36	2754.54	4430.41
19.05	394.85	577.84	1515.45	2950.62	4656.66
25.40	460.97	653.08	1651.65	3324.30	5561.58
			6 × 8 Array		
6.54	422.58	627.78	1541.03	2992.30	4796.92
6.60	455.32	628.83	1632.38	2993.34	4710.84
7.94	427.48	611.72	1513.62	2935.71	4708.50
9.43	426.11	600.00	1513.07	2860.76	4594.37
10.16	435.04	584.81	1477.62	2880.97	4563.58

Mean interface temperature 294 ± 6 K; all pressure values ± 10 kPa.

Table 3 Integrated load configuration test thermal contact conductance values

Apparent pressure, kPa	4 × 6 Array	5 × 7 Array	6 × 8 Array
206.8	215.04	381.80	443.07
344.7	447.82	571.96	622.10
551.6	1090.79	1492.85	1564.81
689.6	2127.66	2844.85	2970.43
827.4	3620.85	4594.67	4729.86

All values in W/m²K.

In order to substantiate the accuracy of the experimental results, the comparisons were made with the experimental data obtained from several previous investigations. The thermal contact conductance for the test pad coated with indium, at an apparent contact pressure of 689.5 kPa (100 psi), compared favorably with other investigators, as illustrated in Fig. 9. Soft metallic coatings on stainless steel and nickel substrates provided a slightly higher value of the thermal contact conductance ratio than the present data. Soft metallic coatings on aluminum or bronze substrates were comparable or slightly below the present data. The temperature of the interface and the thickness of the coating also affect the thermal resistance, with higher temperatures and/or thicker coatings yielding lower values of the conductance ratio. Although not apparent in Fig. 3 or 4, the thermal contact conductance was extremely sensitive to the distance from the load point and, hence, the interface pressure.

Assuming that the optimum load configuration is defined as one that minimizes the number of load points yet maximizes the thermal contact conductance, it would seem that the 5 × 7 array is the best of the three configurations evaluated. This is due to the combination of factors, the most important of which is the density of the load points. Of secondary importance however, is the symmetry of the load distribution. For the 5 × 7 array, the load is distributed over a region that is 2.54 cm by 2.54 cm in size. For the 4 × 6 array, the load region is 2.96 × 3.175 cm, and for the 6 × 8 array, the load region is 2.22 × 2.12 cm.

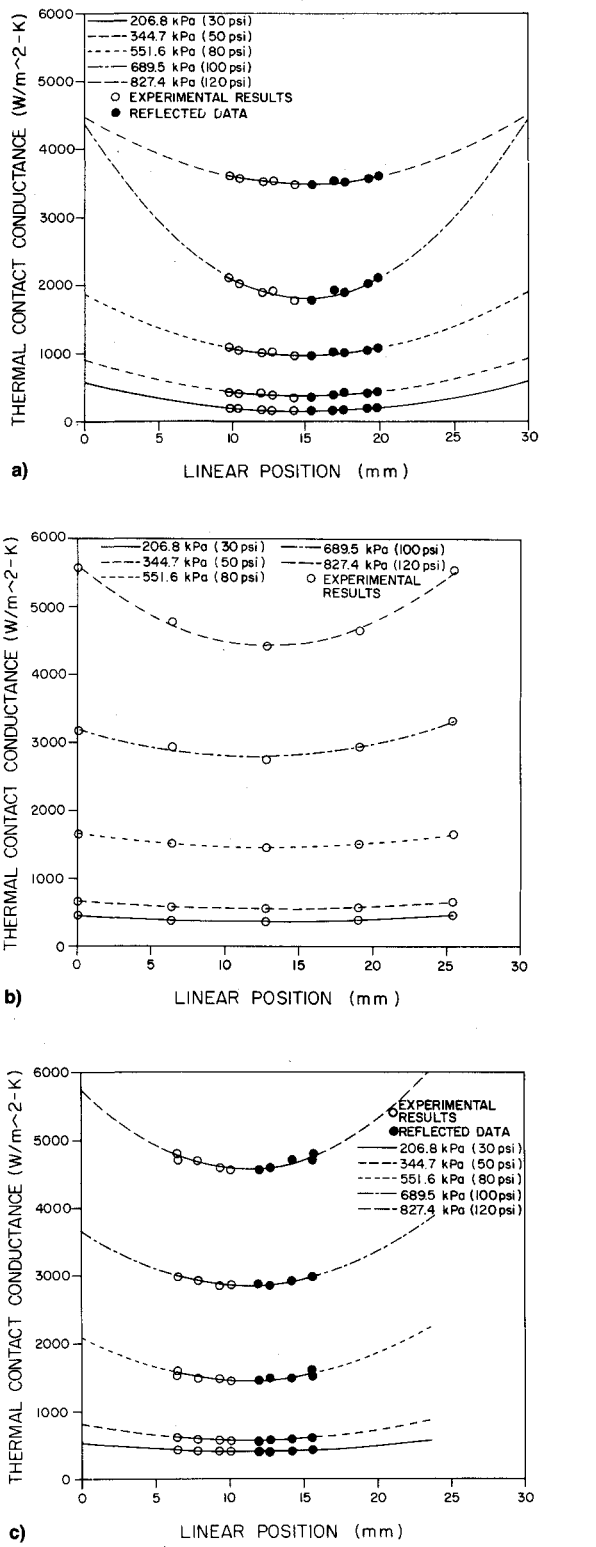

Fig. 7 Thermal contact conductance as a function of position for: a) 4 × 6 load array; b) 5 × 7 load array; c) 6 × 8 load array.

For any plate constructed from a homogeneous material, an optimum spacing exists and this optimum spacing presumably would be identical for both directions. As a result, a configuration that uses symmetrically spaced load points near the optimum value could have a higher average conductance than one that used nonsymmetrically spaced load points. This would be true even if one of the dimensions of the nonsymmetrical distribution was close to the optimum than that of the symmetric distribution, which was thought to be the case here.

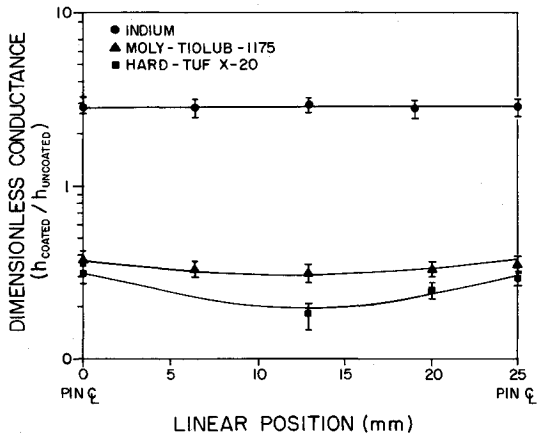

Fig. 8 Dimensionless thermal contact conductance for TTPS-3, -4, and -5 as a function of the distance from a load point.

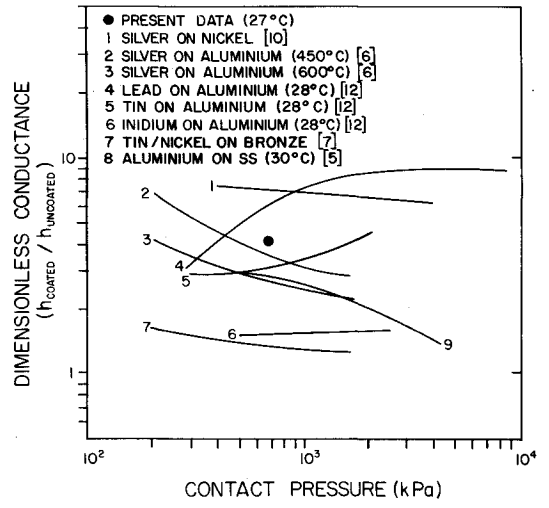

Fig. 9 Comparison of the dimensionless experimental contact conductance data as a function of apparent contact pressure with results from previous investigations.

Conclusions

In this investigation, the pressure distribution of the thermal pad contact heat exchangers was evaluated numerically using a self-contained general purpose finite element program (ANSYS) and experimentally using a relatively new pressure sensitive film manufactured by the Fuji Corporation. Both numerical and experimental analyses of the test pads were conducted for load points in 4 × 4, 4 × 6, 5 × 7, and 6 × 8 arrays.

The numerical investigation provided a reasonable representation of the pressure distribution, and indicated that the interface pressure distribution variation was directly proportional to the total load and decreased with increasing number of load points. Because the sensitivity of the film and the variation of the pressure distribution over the surface of the test pads was of the same relative magnitude as the nonuniformity of the initial test, it was not possible to determine the precise variation of the pressure distribution for the different loading configurations. However, two significant conclusions can be drawn from these results. The first is that, as expected and predicted by the numerical model, the pressure distribution becomes more uniform as the number of the load points increases. Second, also as predicted by the numerical model, the pressure variation increases in direct proportion to the load.

The results of the thermal contact conductance enhancement tests indicated that the thermal contact conductance of the 12.70 × 17.78 cm thermal test pads can be enhanced significantly by the addition of a thin coating of indium. Using similar pressures, the enhancement factor obtained for the indium coated test pair was found to be extremely close to that previously reported in the literature, a factor of 3.8 for an apparent pressure of 689.5 kPa (100 psi) as compared to a factor of 3.5. However, the Moly-Toilub-1175 and Hard-Tuf X20 coated interfaces both resulted in a reduction in the thermal contact conductance by approximately 66% and 77%, respectively.

References

[1]Peterson, G. P., and Fletcher, L. S., "Heat Transfer Enhancement Techniques for Space Station Cold Plates," *Journal of Thermophysics and Heat Transfer*, Vol. 5, No. 3, 1991, pp. 423–428.

[2]Oehler, S. A., McMordie, R. K., and Allerton, A. B., "Thermal Contact Conductance across a Bolted Joint in a Vacuum," Fourteenth AIAA Thermophysics Conf. AIAA Paper 79-1068, Orlando, FL, June 4–6, 1979.

[3]Schwarz, B., "Thermal Interface Conductance on Liquid Cooled Cold Plates for the Spacelab," *Proceedings of the Spacecraft Thermal and Environmenutal Symposium,* Munich, Germany, Oct. 10–12, 1978, pp. 285–292.

[4]Yovanovich, M. M., "Theory and Applications of Constriction and Spreading Resistance Concepts for Microelectronic Thermal Management," *Proceedings of the International Symposium on Cooling Technology for Electronic Equipment,* Pacific Institute for Thermal Engineering, Honolulu, HI, March 1987.

[5]Fletcher, L. S., and Peterson, G. P., "The Effect of Interstitial Materials on the Thermal Contact Conductance of Metallic Junctions," *Proceedings of the Heat Transfer in Thermal Systems Seminar-Phase II,* National Cheng Kung Univ., Tainan, Taiwan, ROC, 1986, pp. 1–8.

[6]Fried, E., and Kelley, M. J., "Thermal Conductance of Metallic Contacts in a Vacuum," AIAA Thermophysics Specialist Conference, AIAA Paper 65-661, Monterey, CA, Sept. 1965.

[7]Mal'kov, V. A., and Dobashin, P. A., "The Effect of Soft-Metal Coatings and Linings on Contact Thermal Resistance," *Inzhenerno-Fizicheskii Zhurnal,* Vol. 17, No. 5, 1969, pp. 871–879.

[8]Shah, H. J., Personal communication, 1978.

[9]Al-Astrabadi, F. R., O'Callaghan, P. W., and Probert, S. D., "Thermal Resistance of Contacts: Influence of Oxide Films," AIAA Fifteenth Thermophysics Conf., AIAA Paper 80-1467, Snowmass, CO, July, 1980.

[10]Negus, K. J., Yovanovich, M. M., and Thompson, J. C., "Thermal Constriction Resistance of Circular Contacts on Coated Surfaces: Effects of Contact Boundary Conditions," AIAA Twentieth Thermophysics Conf., AIAA Paper 85-1014, Williamsburg, VA, June, 1985.

[11]Hegazy, A. A., "Thermal Joint Conductance of Conforming Rough Surfaces: Effects of Surface Microhardness Variations," Ph.D. Thesis, Univ. of Waterloo, Ontario, Canada, Mechanical Engineering Dept., 1985.

[12]Antonetti, V. W., "On the Use of Metallic Coatings to Enhance Thermal Contact Conductance," Ph.D. Thesis, Univ. of Waterloo, Ontario, Canada, Mechanical Engineering Dept., 1983.

[13]Kang, T. K., Peterson, G. P., and Fletcher, L. S., 1989, "Enhancing the Thermal Contact Conductance through the Use of Thin Metallic Coatings," American Society of Mechanical Engineers/American Institute of Chemical Engineers National Heat Transfer Conf., ASME Paper 89-HT-23, Philadephia, PA, Aug. 5–8, 1989.

[14]Aron, W., and Colombo, G., "Controlling Factors of Thermal Conductance Across Bolted Joints in a Vacuum Environment," American Society of Mechanical Engineers Winter Annual Meeting, ASME Paper 63-WA-196, Philadelphia, PA, 1963.

[15]Madhusudana, C. V., Peterson, G. P., and Fletcher, L. S., "The Effect of Non-uniform Pressures on the Thermal Conductance in Bolted and Riveted Joints," *ASME J. Energy Resources Technology*, Vol. 112, No. 3, September, pp. 174–182.